Available online at www.sciencedirect.com
SCIENCE DIRECT®
Surface Science 555 (2004) 145–156
SURFACE SCIENCE
www.elsevier.com/locate/susc

Acetic acid adsorption and decomposition on Pd(1 1 0)

Michael Bowker *,[1], Chris Morgan [1], John Couves [2]

Centre for Surface Science and Catalysis, Department of Chemistry, University of Reading, Whiteknights Park, Reading RG6 6AD, UK

Received 10 September 2003; accepted for publication 19 December 2003

Abstract

The reaction of acetic acid with Pd(1 1 0) has been investigated using temperature-programmed desorption (TPD) and a molecular beam reactor. The sticking of acetic acid is very efficient and results in hydrogen evolution and acetate formation at room temperature. The acetate decomposes between 320 and 440 K to produce CO_2 and hydrogen coincidently and leaves C adsorbed on the surface. The presence of carbon results in a changed desorption profile after readsorbing acid on the surface, manifesting an autocatalytic decomposition profile, with a half-height width of as low as 9 K and a slowed decomposition rate (higher peak temperature). Surprisingly, at higher temperatures where the acetate is unstable (>450 K), the sticking of acetic acid continues at a steady-state rate and is not poisoned by the build-up of C on the crystal. This is due to the fact that most of the C deposited is lost from the surface to the bulk in a facile manner above about 450 K, leaving a reactive surface which is apparently continually available for decomposition. The reactive surface appears to be Pd(1 1 0) with 0.5 monolayers of C adsorbed in the c(2×2) structure, which acts as a template for increased stability and ordering of the acetate adlayer.

Keywords: Molecule–solid reactions; Adsorption kinetics; Catalysis; Chemisorption; Surface chemical reaction; Palladium; Carboxylic acid; Sticking

1. Introduction

The selective oxidation of olefins by palladium is important both synthetically and industrially. Vinyl Acetate (VA) is an important petrochemical intermediate used in the manufacture of adhesives, paints and coatings. The industrial VA process was originally developed in the 1960s [1,2] and was based on the homogeneously catalysed reaction of ethylene with acetic acid, using palladium and copper chloride catalytic system. This was later replaced by a heterogeneous catalyst system based on a supported palladium catalyst.

$$CH_3COOH + C_2H_4 + \tfrac{1}{2}O_2 \longrightarrow \text{vinyl acetate} + H_2O$$

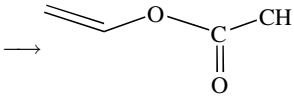

Hoechst [3] and Bayer [4] both developed industrial processes in the late 1960s, the former being based on a palladium-only and the latter on a palladium–gold bimetallic system. The heterogeneous

* Corresponding author. Tel.: +44-2920870120; fax: +44-2920874030.
E-mail address: bowkerm@cardiff.ac.uk (M. Bowker).
[1] Now at Chemistry Department, Cardiff University, P.O. Box 912, Cardiff CF10 3TB, Wales, UK.
[2] BP Chemicals, Sunbury-on-Thames, Middlesex TW17 7LN, UK.

0039-6028/$ - see front matter © 2004 Published by Elsevier B.V.
doi:10.1016/j.susc.2003.12.040

gas phase process has many advantages over the homogeneous process, such as the reduced corrosion, reduced by-product formation and elimination of chloride from the process. Despite the development of the commercial process in the late 1960s there have been few detailed studies of the system [5–8]. This probably relates to the complex nature of the catalyst and the difficulty of handling the reactants. The fundamental interactions of acetic acid with palladium surfaces are not well understood.

The interaction of acetic acid is academically interesting because it is a simple molecule which nevertheless can decompose on surfaces in complicated and unusual ways [9–18] and which usually bonds in a bidentate fashion to the surface through both oxygen atoms [18,19]. It tends to sit on (1 1 0) surfaces in an upright manner as shown by Woodruff [20] and Bonzel [21] using angle resolved photoelectron diffraction, although it has been suggested that monodentate may exist on Pd(1 1 1) at low temperature from HREELS [22], in contrast to earlier findings [19]. The reaction with group 9 and 10 surfaces generally tends to occur in the following manner involving dehydrogenation and C deposition on the surface [9–15].

$$CH_3COOH \rightarrow CH_3COO_a + H_a \quad (1)$$

$$CH_3COO_a \rightarrow C_a + 3H_a + CO_2 \quad (2)$$

$$2H_a \rightarrow H_2 \quad (3)$$

In comparison to the much more studied formic acid, acetic acid is a weaker acid and so the conjugate base, the acetate, is a stronger base than the formate and tends to higher stability on the surface. Thus on Cu(1 1 0) it decomposes at 600 K [15–17], whereas the formate decomposes at about 450 K [23,24], while on the more reactive Pd(1 1 0) surface acetate decomposes at ~350 K [13,14], but the formate breaks down at ~230 K [25]. Further, the acetate tends to show very different kinetic behaviour. Often the formate manifests near-ideal first-order decomposition kinetics in TPD [15–17], but on a variety of surfaces the acetate shows somewhat anomalous behaviour. This was first described by Madix et al. for Ni single crystal surfaces [9]. They christened this behaviour a 'surface explosion', a type of autocatalytic phenomenon [26]. There was then a gap in interest and findings in this area until the 1990s when the effect was 'rediscovered' for a variety of surfaces [11–15,27–30] and it was even identified to occur on high surface area, nanoparticulate, supported Rh catalysts [27,28]. Thus this adsorbate presents us with an interesting system to study, partly because the details of the kinetics of its decomposition are not fully resolved.

The aim of the present work was to attempt to shed new light on this phenomenon by combining TPD methods with isothermal molecular beam reaction measurements and with kinetic modelling. Particularly important questions relate to the role of coadsorbates and of surface structure in the decomposition kinetics. Further, this is one part of a programme aimed at understanding industrial vinyl acetate synthesis at the molecular and surface level.

2. Experimental

A schematic of the ultra-high vacuum (UHV) system used in this work is given in Fig. 1. It comprises a stainless steel UHV chamber maintaining a base pressure of $\sim 2\times10^{-10}$ mbar (95% H_2) which increased to $\sim 6\times10^{-10}$ mbar during the adsorption experiments. The Pd(1 1 0) crystal was mounted on a custom-built holder in the chamber centre. In the same horizontal plane are the molecular beam enclosure, a rear-view optics system with a coaxial electron gun (supplied by VG) for low energy electron diffraction (LEED) and Auger electron spectroscopy (AES), and a set of differentially pumped chambers which comprise an angle resolved mass spectrometer. Also in the main UHV chamber is a quadrupole mass spectrometer (QMS) (Hiden Analytical Limited) employed for residual gas analysis (RGA). The QMS provides an indication of the angle-integrated partial pressure within the vacuum chamber, since no direct line of sight exists between the sample and detector.

The Pd(1 1 0) crystal (5 N purity, Metal Crystals and Oxides Ltd.) cut and polished in the (1 1 0) plane could be heated and cooled in the chamber

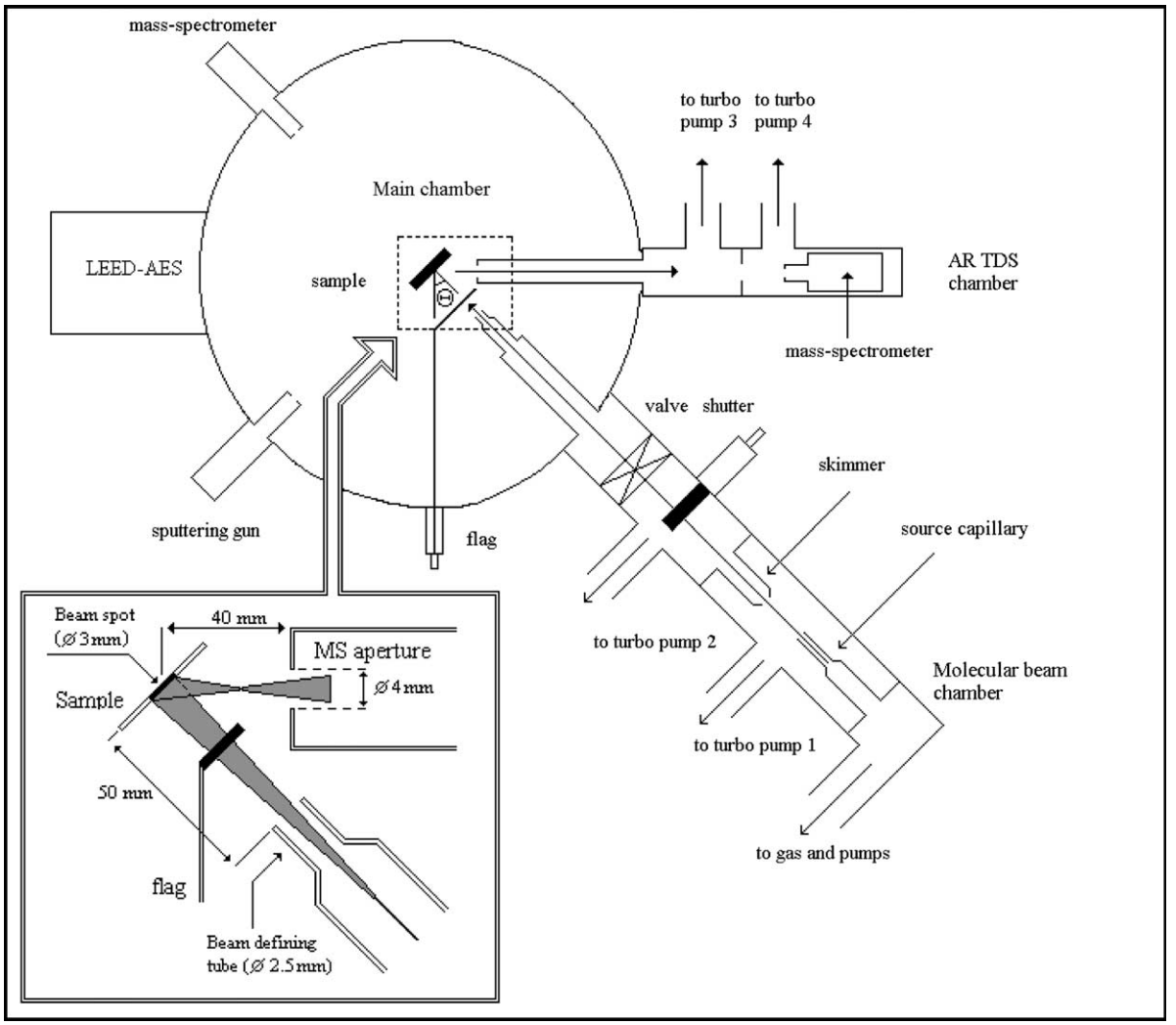

Fig. 1. Schematic diagram of the molecular beam system and UHV analysis chamber.

to between 1040 and 110 K. The sample was heated by direct contact with two tungsten wires, which passed through grooves in the edge of the crystal and were resistance heated. The heating rate was set at 1 K s^{-1} in the temperature range of interest. Sample cooling was performed by close proximity of the sample mount to a liquid N_2 reservoir, connected by a Cu braid and a sapphire thermal switch. Temperature was recorded through a chromel–alumel thermocouple attached to the sample by a small hole drilled in the edge parallel with the surface plane. The surface was cleaned by cycles of Ar^+ bombardment (500 eV, 6 $\mu A/cm^2$, 30 min), annealing (850 K, 20 min) and flashing (1020 K, 2 min) as documented elsewhere [29–34]. The major elemental impurities in Pd-(1 1 0), S and C, were removed during the sputtering cycles. The absence of S was determined by AES, but this was less useful for determining carbonaceous contamination due to the overlap of C (275 eV) and Pd (283 eV) Auger peaks. As an alternative, O_2 dosing, followed by TPD was used to check for the presence of CO and CO_2 in the desorption trace [35,36]. Also, CO TPD proved

useful for detecting C contamination through analysis of the α3 peak at low temperatures [36–38]. In addition, a sharp (1×1)-Pd(1 1 0) LEED pattern indicated a well-ordered surface. LEED patterns were observed using rear-view optics (VG Microtech). Between successive TPD exposures to acetic acid, the Pd(1 1 0) surface was heated in O_2 to remove C from the surface. For TPD analysis, acetic acid and oxygen were dosed via a leak valve through a narrow stainless steel dosing tube, pointed at the sample.

The use of a molecular beam reactor system allows sticking and kinetic information to be obtained, and is described in more detail in previous literature [39]. The system relies on principles originally presented by King and Wells [40], removing problems associated with mass spectrometer calibration and enabling sticking probabilities to be measured to within ±0.01. Although the sticking of simple molecules can be obtained in this way, this was not possible for acetic acid. This is because this is a reflection technique and measures the total scattered flux in the chamber and acetic acid, once reflected off the crystal tends to stick to the walls at which it impinges. It thus does not register a significant pressure rise in the arrangement used here (the mass spectrometer is situated out of line-of-sight with the sample). We hope to change the arrangement in the future for this purpose. An in-beam pressure of $\sim 1.0\times10^{-7}$ mbar is obtained from a source pressure of 20 mbar. The beam impinges on the crystal surface to give an exposure disc of 2.9 mm diameter. The liquid glacial acetic acid source (~100%, BDH) was cleaned by repeated freeze–pump–thaw cycles before a beam experiment was performed. To prevent decomposition in sunlight, all liquids were kept in covered glass vials. The purities of gaseous Ar (99.999%, Argo Ltd.) and O_2 (99.6%, Argo Ltd.) were considered to be of a suitable level for direct use.

3. Results and discussion

3.1. Temperature-programmed desorption

Fig. 2 shows the product evolution after dosing acetic acid onto the Pd(1 1 0) surface at 220 K.

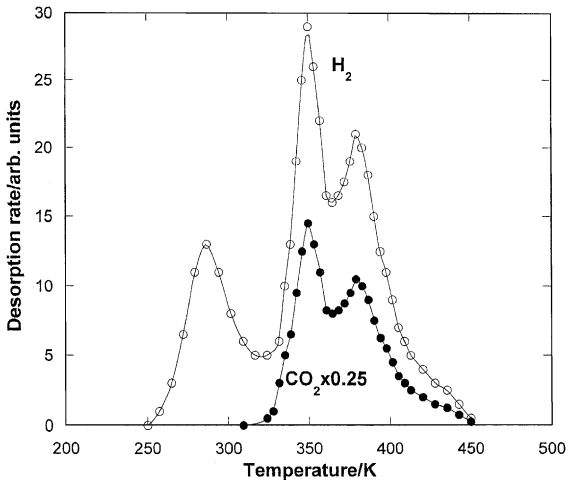

Fig. 2. TPD from the clean surface dosed with 2 L of acetic acid at 220 K, showing products from acetic acid decomposition.

Hydrogen is evolved in a desorption-limited peak at 290 K, followed by CO_2 and hydrogen produced almost coincidently in a double-peaked structure between 325 and 400 K. The latter are due to acetate decomposition, for which the rate determining step in product evolution is the decomposition step itself (not desorption), whereas the 290 K peak is due to recombination of the earlier dissociated acid hydrogens from the carboxylic acid. The products are as outlined in reactions 1 and 2 above, giving CO_2 and H_2 in the gas phase, which must leave the C from the methyl group of the acetic acid on the surface. As a result the TPD is not then reproducible unless the surface is once again cleaned by sputtering and annealing. If this is not done and the C is present on the surface during adsorption, then this has dramatic consequences for the desorption as outlined in Fig. 3. In this case the sample was only heated to 520 K during the desorption experiment, was then cooled and re-exposed to 2 L of acetic acid. The adsorption is carried out at 323 K and so the first desorption curve in this sequence is similar to that in Fig. 2, except the first peak is not quite so big, presumably due to a little decomposition of the acetate at this temperature of adsorption. As the experiment is repeated, so the peaks change to essentially one desorption state at higher temper-

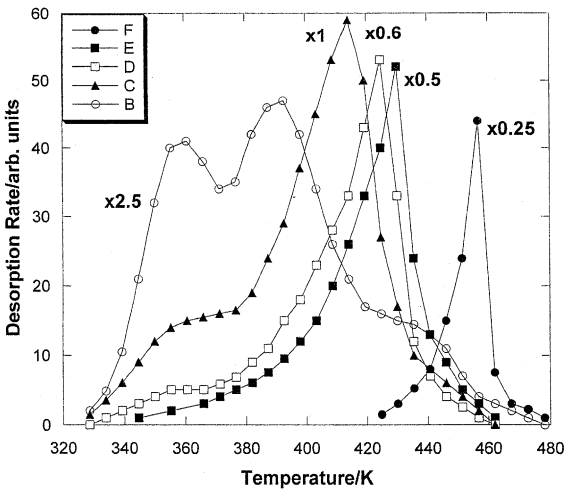

Fig. 3. TPD (at 44 amu) from the clean surface dosed with 2 L of acetic acid at 323 K, followed by repeated doses and TPD, after heating each time to only 530 K. The first TPD is curve B, the second curve C, the third curve D, while curve E is the 6th dose and desorption. Curve F is a new experiment for which the surface was dosed with 12 L acetic acid at 473 K, which deposits C on the surface, followed by 2 L at 323 K.

ature than before. The biggest shift in the temperature is between the first experiment and the third, there is only a slight shift on re-dosing three more times. As the experiment is repeated, so also the peak gets much narrower, from approximately 32 K FWHM for curve C to about 20 K for curve E. If we carry out a further experiment, which involves dosing 12 L of acetic acid at 473 K (and therefore decomposing it to leave carbon on the surface), followed by re-dosing 2 L of the acid at 323 K as before, then we see a significant further increase in peak temperature to 452 K, and narrowing of the peak to only 10 K wide, a very definite surface explosion type of desorption. Thus the acetate appears to be stabilised by the presence of C on the surface. Indeed, it is likely that the second decomposition peak at 380 K in Fig. 2 may occur due to C deposition occurring with the first peak at 350 K. Experiments with CO dosing showed that the saturation coverage at 320 K dropped by approximately a factor of two, and that the peak temperature for CO decreased from 450 to 430 K after dosing acetic acid to form the c(2×2) described in the following sections. The structure of the C layer on which the stabilised acetate rests is addressed below.

The narrowing of the desorption can be attributed to an autocatalytic surface event, as originally described by Madix [9,41,42] and more recently by ourselves [10–14,27,28]. Although the peaks are narrow in Fig. 3, note they are not as narrow as they can be on other surfaces. On Rh(1 1 0) the peak width can be as small as 5 K [11], while the narrowest width of ~6 K reported by Madix et al. was obtained for formic acid [32,33] and acetic acid [9] on Ni(1 1 0). We consider this unusual desorption process to be an homogeneous second-order autocatalytic phenomenon [28,43]. If the desorption curve with the highest peak temperature in Fig. 3 is analysed in the normal Arrhenius fashion, that is, described by the normal rate equation (I) given below, then unrealistic kinetic parameters are obtained, as shown in Table 1. This is due to the fact that this is not a NORMAL desorption process, it is autocatalytic, and the appropriate equation for this is given below (Eq. (II)).

Normal Arrhenius rate equation

$$-\mathrm{d}\theta/\mathrm{d}t = A \cdot \theta \cdot \exp(-E/RT) \qquad \text{(I)}$$

For classical desorption the desorption activation energy, E, can be determined from a plot of ln rate vs. reciprocal temperature for rates measured at the low temperature side of the normal desorption curve, where θ is essentially constant. Modelled TPD spectra for such a situation are shown in Fig. 4a and b. In Fig. 4a we have simulated TPD spectra with desorption parameters of 100 kJ mol^{-1} activation energy and an A-factor of 10^{14} s^{-1}. It can be seen that the Arrhenius plot in Fig. 4b gives a reasonable straight line at the low coverage side of the TPD curve (high $1/T$), which yields the correct activation energy and A-factor (that is, those input to the modelling program) upon analysis (see Table 1). For an autocatalytic process the rate equation is quite different:

Autocatalytic rate equation

$$\mathrm{d}\theta/\mathrm{d}t = A \cdot \theta \cdot (1-\theta) \cdot \exp(-E/RT) \qquad \text{(II)}$$

Table 1
Desorption experiment and modelling

Desorption type	Analysis	E (kJ mol^{-1})	A (s^{-1})	T_p (K)	$W_{1/2}$ (K)
Modelled normal kinetics					
Fig. 4a		100	10^{14}	355	25
Fig. 4b	Arrhenius	100	10^{14}		
	Redhead	102	10^{14*}	355	
Modelled autocatalytic					
Fig. 4c		100	10^{14}	355–374	5–25
Fig. 4d	Arrhenius	190	5×10^{25}	374	
	Redhead	106	10^{14*}	374	
Experiment (Fig. 3F)				456	10
	Arrhenius	185	2×10^{20}	456	
	Redhead	130	10^{14*}	456	
		124	10^{13}	456	
Experiment modelled with autocatalytic kinetics (Fig. 5)	$\theta_0 = 0.98$	118	10^{13}	456	10

Now, in this case, at the low temperature end of the desorption curve $(1-\theta)$ may be very small, but increases very significantly with temperature as the desorption proceeds at high θ. Thus the exponential term is not the only variable in this case as the temperature increases near the beginning of the desorption process; $(1-\theta)$ also increases very fast. A model example of these differences between the two approaches is given in Fig. 4, 4c and 4d being for autocatalytic kinetics governed by Eq. (II), and indicates why the anomalous values of the A-factor and activation energy are obtained from the normal analysis. The Arrhenius plot is actually curved (Fig. 4d), and so a straight line for E determination can only be approximated. In fact a far better estimate of the desorption activation energy is obtained from the Redhead method [44] assuming an A-factor of 10^{14} s^{-1} and then deriving the activation energy. This gives the values shown in Table 1, which are in reasonable agreement with the real activation energy shown in Table 1 (final row) derived from analysis of the experimental data using the proper autocatalytic kinetics as follows. We have used a computer model of such kinetics (based on Eq. (II) above) to simulate the experimental decomposition, with the values shown in Table 1 and the resulting desorption curve is shown in Fig. 5 and this gives a reasonable fit to the data. It must be noted, however, that the desorption profile and half width are *strongly* dependent on conditions, particularly temperature and time of dosing, both of these strongly affecting the amount of surface C deposition which induces the surface explosion. Further, both the pre-exponential factor and the starting coverage for the desorption modelling strongly affect the peak width, and so, since the starting coverage is not known *exactly*, the fitting has only been carried out in a semi-quantitative way. The peak temperature and width are good fits, but the overall shape is somewhat worse.

Note that this model is essentially the same as that proposed by Madix et al. [9,41,42], but the mechanistic source of the kinetics is somewhat different. We consider that the reaction occurs by the decomposition of acetates at vacant adjacent sites (Madix's initiation sites), which are low in coverage at the beginning of the desorption. The process is mediated by a mobile system in which the vacancies in the adlayer formed by acetate decomposition diffuse fast and are randomised, and of an average homogeneous distribution throughout the process. The difference with Madix's original model is very little, although the importance of islands of adsorbate was stressed in that work. Perhaps the most important difference is that we have shown that explosive decomposition is only ever observed *in the presence of a co-adsorbate*. Thus on Rh(1 1 0), the explosion was

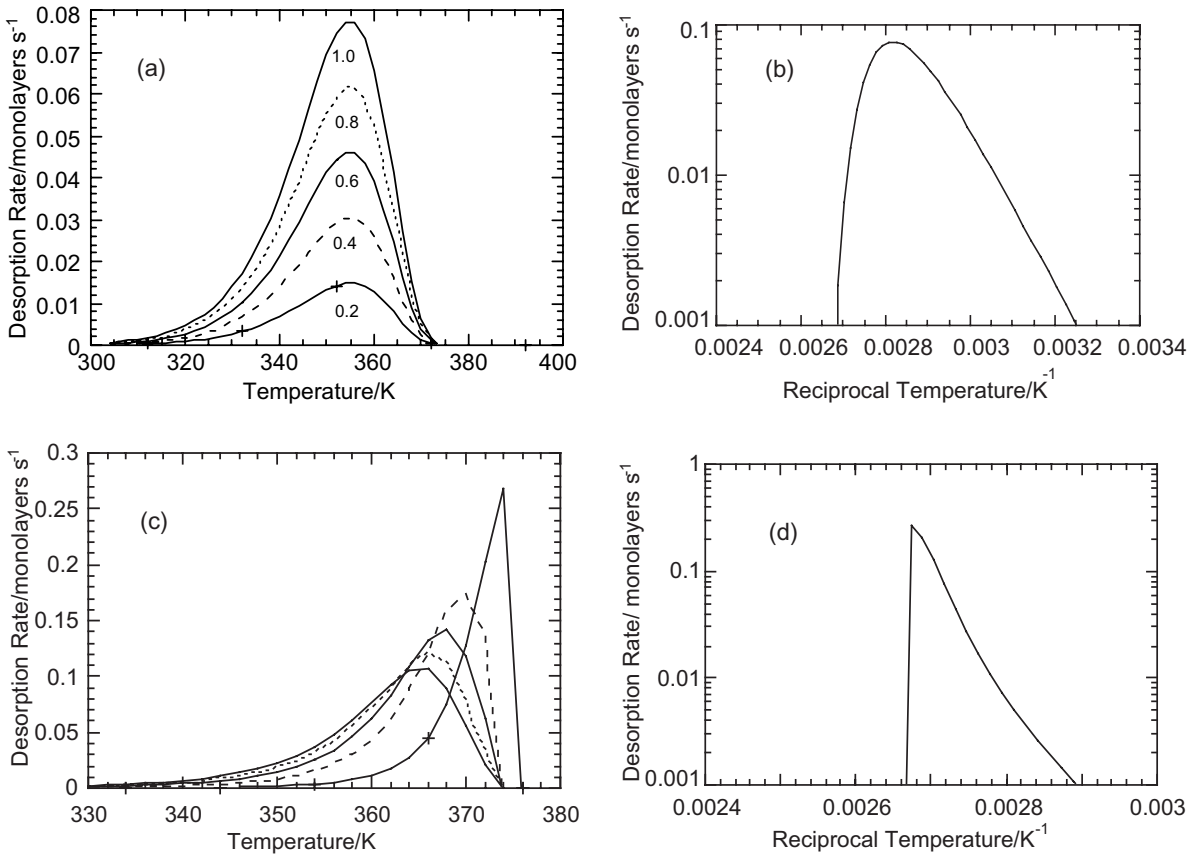

Fig. 4. Modelled TPD, showing the difference between normal and explosive decomposition kinetics. Plot a is for classical first-order desorption kinetics for coverages between 0.2 and 1.0 monolayers ($A = 10^{14}$ s^{-1}, $E = 100$ kJ mol^{-1}), while b is an Arrhenius plot of these data for the 1.0 monolayer curve, showing near linearity at low temperature (high coverage). Plot c is modelled TPD for a coverage of around 0.99 monolayers, with the same Arrhenius parameters, but with explosive kinetics, while plot d is the equivalent Arrhenius plot. It is clear that the Arrhenius plot is not linear, but the low temperature edge gives the parameters shown in Table 1. The actual coverages used in c are from 0.987 monolayers from the lowest temperature peak to 0.999 monolayers for the highest temperature peak, in steps of 0.003 monolayers additional coverage.

observed when either C, N or O was predosed [11], but not without them. Although it is not completely clear what the role of such coadsorbates is, it is possible that they act as stabilisers for the exploding intermediate by blocking active sites for the decomposition, which are represented by the $(1-\theta)$ term in (II) above. Thus in reference to Madix's work we propose that a coadsorbate was also responsible for this effect and that this may have been C or CO formed during the initial stages of the decomposition at high coverages of adsorbate. The model of the process is discussed in more detail below.

3.2. Molecular beam and LEED studies

We have carried out reaction rate measurements using the molecular beam reactor described elsewhere [39,45] and the results for a variety of adsorption temperatures on an initially clean surface are shown in Fig. 6. The significant points are that only hydrogen is seen as a product below ~320 K, whereas at higher temperatures CO_2 is seen to evolve coincidentally with the hydrogen. TPD experiments were carried out after each of these molecular beam runs and the TPD width varied between 10 and 25 K. The signal to noise

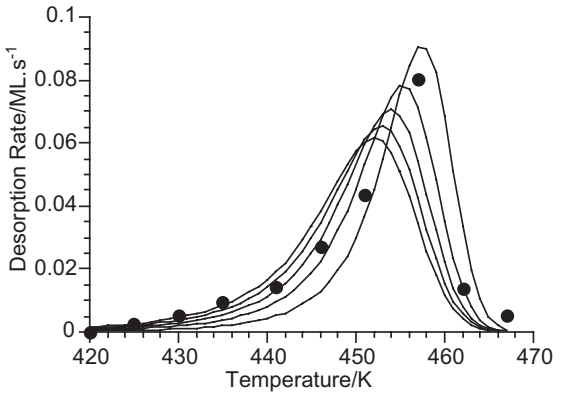

Fig. 5. Modelling of the experimental TPD, the parameters used are shown in Table 1. Data points are the experiment while the solid lines are the modelled curves using autocatalytic kinetics using Eq. (II) in the text and starting coverages ranging from 0.95 to 0.99 (highest temperature peak) of the maximum coverage.

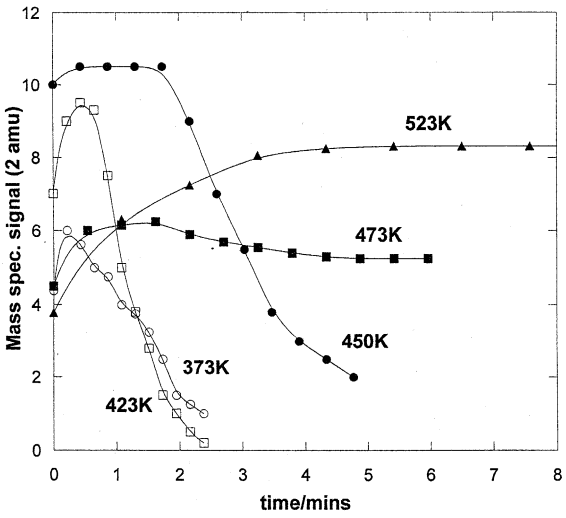

Fig. 6. The hydrogen production during reaction of acetic acid with clean Pd(1 1 0) at different crystal temperatures. The reaction appears to be continuous above 450 K or so. In subsequent TPD experiments after the conclusion of these runs acetate decomposition was identified for the two lowest temperature experiments, but none was present for the 450 K experiment and higher temperatures.

ratio in this case was somewhat worse than above because the beam area is approximately 7% of the total crystal area. For higher adsorption temperatures the desorption peak was shifted to higher temperature (for 373 K adsorption it was 430 K, for 423 K it was 475 K). Desorption was no longer seen after the beam experiment when the temperature during dosing was >450 K; instead, steady-state decomposition of the acetate was observed. This is somewhat surprising since C atoms from the methyl group of the acetate are continually being deposited during such an experiment; it would be expected that the decomposition would be poisoned once a significant fraction of a monolayer was formed. The fact that the reaction proceeds under these circumstances (and we have measured the same steady-state rate after approximately 10 monolayers of C have been deposited) indicates that the carbon leaves sites at the surface unaffected, probably because it diffuses subsurface. This must already be occurring at 450 K, indicating a very facile diffusion of C into the Pd lattice. This C is easily removed again by introducing O_2 into the beam after removing the acetic acid, as shown in Fig. 7. It is clear that oxygen can adsorb readily on this layer, notwithstanding the presence of the carbon. The oxidation of the carbon clearly proceeds in two phases, with initial CO production desorbing as CO when the carbon coverage is high and the oxygen coverage is low, followed by CO_2

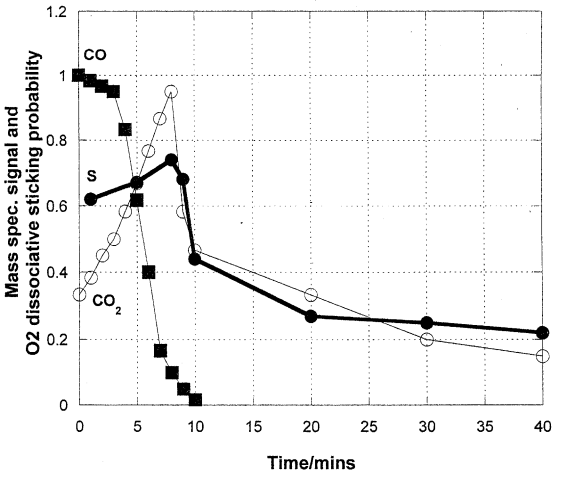

Fig. 7. Showing a carbon clean-off experiment using an oxygen molecular beam. The surface was first exposed to acetic acid for 15 min at 473 K, the oxygen being then introduced at time zero on the plot. The product observed immediately is CO, followed by CO_2.

production due to secondary reaction of surface CO with surface oxygen, when the opposite is the case. At the lower adsorption temperatures (<450 K) where the acetate is stable and the adsorption and decomposition ceases, it is clear that the acetate is adsorbed on a carbonaceous layer since the decomposition temperature is increased from that on the clean surface.

We have carried out display LEED experiments to parallel the beam experiments, particularly in order to establish the state of the surface upon which steady-state acetic acid decomposition takes place, that is, is there an ordered or disordered surface layer of C, or is the surface clean? There is no evidence of order in the LEED after dosing acetic acid on to the clean surface (Fig. 8a) at room temperature, just a (1×1) pattern with a high background intensity. However, if we carry out LEED after dosing 5 L acetic acid at 473 K, then a clear c(2×2) LEED pattern is obtained (see Fig. 8b). This is due to adsorbed C since neither the acetate nor CO are stable for the length of the LEED experiment at this temperature. The question remains as to whether the steady-state catalysis takes place on this c(2×2)-C layer, that is, is the C layer stable at elevated temperature? The LEED evidence appears to show that it is. Thus the catalysis takes place on top of this ordered C structure (for instance, for the 473 K experiment in Fig. 6) and the acetate is adsorbed on it for the final experiment in Fig. 3 for example. If the acetate is formed by adsorption of acetic acid at 373 K on a c(2×2)-C layer previously formed at 473 K, then an ordered c(2×4) structure is formed (Fig. 8c), though the acetate is presumably bound to Pd metal atoms. The same structure can be obtained by dosing acetic acid at 400 K, presumably because the C layer forms first due to the initial decomposition of the acetate before it is stabilised by the carbon layer. This structure is somewhat unstable if adsorbed at around 420 K, so that mixed c(2×2) and c(2×4) are often seen,

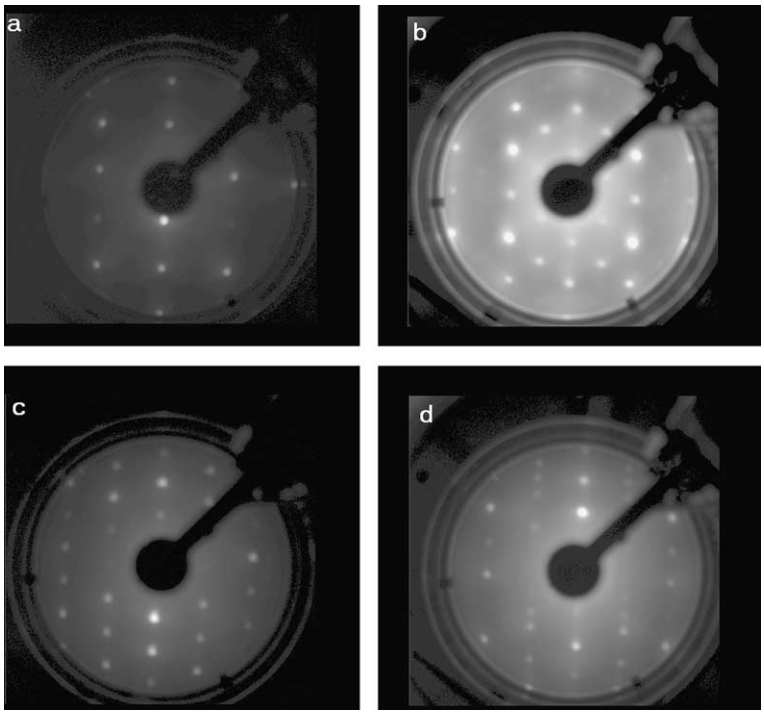

Fig. 8. LEED patterns observed during acetic acid treatments. (a) Clean surface (124 eV); (b) c(2×2) after acetic acid dosing at 473 K (157 eV); (c) c(2×4) after acetic acid adsorption at 373 K onto a preformed c(2×2)-C surface layer (62 eV); (d) mixed c(2×2), c(2×4) structure observed at 423 K (64 eV).

and if left a long time produces the c(2×2) structure, presumably due to acetate decomposition (Fig. 8d); there may also be some electron beam-enhanced decomposition in such cases. The extra C accumulated during the steady-state reaction shown in Fig. 6 is thus lost from the active area, presumably by dissolution into the bulk of the crystal. Auger measurements are difficult because the C(KLL) and Pd(MNN) at ~270 eV overlap. However, we estimate from the Auger signal ratio that the C coverage is 0.7 (±0.4), though there is no increase in the C signal after high exposures of acetic acid at elevated temperature when we know that several monolayers equivalent of C have been deposited. Although the catalysis takes place on a surface with about 0.5 monolayers of C adsorbed, that C apparently has little negative effect on the rate, and the surface is still very active. In fact there is little obvious decrease of the adsorption probability for acetic acid during such experiments. Thus it is probable that many of the Pd metal surface atoms are still available for acetate binding and reaction. From the LEED alone it is difficult to assign a detailed structure to the adsorbed layer. It consists of a mixed layer of adsorbed carbon and acetate, and it is likely that some reconstruction of the surface is involved, as it is for formate on Cu(1 1 0) [46] and for the c(2×4)-oxygen structure on Pd(1 1 0) [47–49]. It may be that the C atoms are effectively 'subsurface', or in the channels of the (1 1 0) surface and so do not interfere with acetate binding directly. We intend to carry out STM imaging of these adsorbed layers in the future, to gain greater insight into their atomic level structure. Our estimates of surface C coverage would benefit from the use of a more accurate surface analysis method, such as XPS, since we currently can only estimate the saturation coverage as ~0.5 monolayers. It would be very useful to correlate the shift of the acetate decomposition peak with the exact surface coverage of carbon.

3.3. Model of the reaction and catalytic relevance

The model of the way the explosion takes place is as shown in Fig. 9. In the left panel we show the acetate structure on the clean surface. Acetate (shown as the bar) likes to bind to two adjacent metal sites, but during random adsorption it is not possible to fill the sites on the surface marked as dotted circles. This is because two free sites are needed for acetate adsorption and binding, whereas this is a single, isolated metal site. As a result this can act as an active site for subsequent decomposition of adjacent acetates when the surface is heated during TPD. Note that the number of such free, isolated sites has here been exaggerated. It is not necessary to have very many to yield pseudo-first-order behaviour. In the right hand

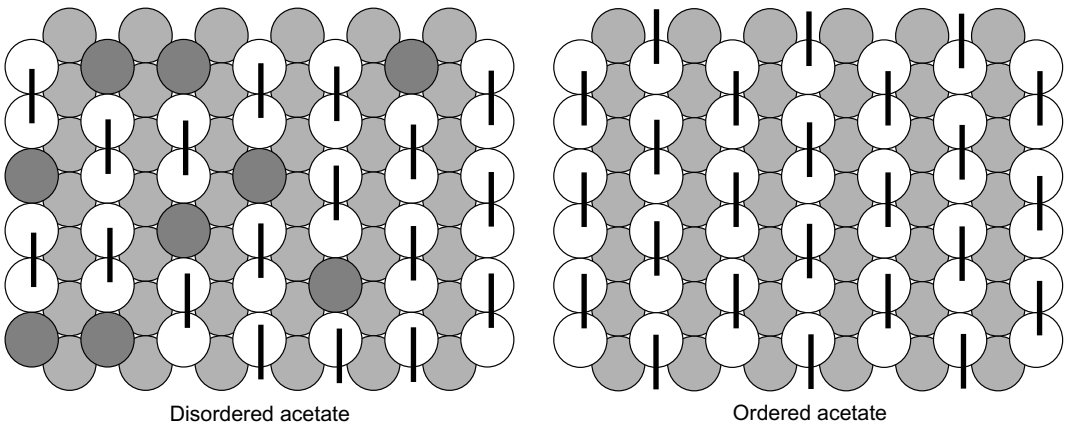

Fig. 9. Schematic models of the surface layer after acetic acid adsorption on the clean surface (left panel) and the C covered surface (right panel), with acetate being shown bound to two adjacent surface Pd atoms. The figure simply shows much more order for the coadsorbed surface, though the detailed structure of this system is not yet known.

panel the acetates are highly ordered and there are no single isolated sites. As a result there is a retarded acetate decomposition and, once free sites appear, 'explosive' decomposition occurs. Note that the structure of the acetate has not been determined in this work and that it is likely that it is adsorbed on a surface which is restructured by the presence of carbon, but is still likely to be bound to two adjacent surface Pd atoms. Our lack of ability in this work to tie down the surface coverage and structure of the C layer makes these proposals only tentative ones.

Since this is an autocatalytic phenomenon, the reaction step itself produces more of one of the components essential to the reaction. In terms of acetate decomposition this can be written as

$$CH_3COO_a + S \rightarrow \tfrac{3}{2}H_2 + CO_2 + C_a + 2S$$

thus the reaction is autocatalytic because the surface concentration of active sites, S, *increases* during the course of the decomposition and this is involved in the rate equation for the decomposition reaction; S is represented by the $(1-\theta)$ term in Eq. (II) above. This is a little surprising in view of the fact that C_a is also produced, which might be expected to block sites. However it is clear that C_a is also *necessary* to give the surface explosion. Our view of this is illustrated in Fig. 9, that is, although C is produced, it only blocks one site, whereas acetate decomposition reveals two new sites; further, it appears that the extra C so produced is lost to the bulk above ~450 K. This is reasonable in light of the fact that carboxylates are bidentate on the surface, binding to two surface atoms [20,21]. However, why another adsorbate (probably atomic) is required is not obvious. The most likely explanation is that such species act as a template for the ordering of the adsorbate layer into structures which result in self-blocking of the decomposition reaction, as proposed earlier [10–12]. It is clear that an ordered c(2×4) acetate structure is formed when the c(2×2)-C structure is present; thus the C layer does seem to act as a template for ordering the acetate. Without the coadsorbate the acetate will be more disordered, adjacent to empty sites in many cases (Fig. 9), and so decomposition will be relatively easy (i.e. the $(1-\theta)$ term in Eq. (II) is never very small). Although the reaction above would still apply in that case, the kinetics are relatively little affected because the term $(1-\theta)$ in Eq. (II) above changes *relatively* little at the low temperature end of the desorption curve. If the number of free sites is very low, then $(1-\theta)$ changes by orders of magnitude early in the desorption process.

Regarding the relevance of these findings to industrial catalysis, let us focus only on the vinyl acetate synthesis reaction, which takes place at a temperature of 420–460 K. The most important finding here is that the most stable surface intermediate formed from acetic acid adsorption, and therefore also likely to be the most abundant surface intermediate (MASI) in the reaction, is the acetate. The coverage of the surface by atoms of either C or O is likely to be very high, and so the acetate is likely to be in the stabilised, explosive state. We have already shown that this explosive state can also be identified on small metal particles of a Rh/alumina catalyst, if the experiment is carried out in a careful way [27,28], and so can probably be observed also on Pd catalysts. It is not clear yet whether there will be a significant C coverage under high pressure conditions, due to the ease of the C clean-off reaction, but C deposition and its loss to the bulk may be a consideration in the design of such catalysts and Au addition may have a role to play here in altering the kinetics and even the occurrence of this reaction. In future work we plan to examine the effect of gold on acetate formation and stability, since commercial catalysts for this reaction contain both Pd and Au.

Acknowledgements

The authors are very happy to thank EPSRC and BP Chemicals for the award of an Industrial Case studentship to CM.

References

[1] I. Moiseev, M. Vargaftic, Ya. Syrkin, Dokl. Akad. Nauk. USSR 133 (1960) 377.
[2] Chem. Week 101 (1967) 73, British Patent 964001, 969162.

[3] Eur. Chem. News 11 (1967) 40.
[4] World Pet. Cong. Proc. 5 (1968) 41.
[5] E. Crathorne, D. Macgowan, S. Morris, A. Rawlinson, J. Catal. 149 (1994) 254.
[6] D. Kragten, R.A. van Santen, M. Crawford, W. Provine, J.J. Lerou, Inorg. Chem. 38 (1999) 331.
[7] S. Nakamura, T. Yasui, J. Catal. 23 (1971) 315.
[8] W. Provine, P. Mills, J.L. Lerou, Stud. Surf. Sci. Catal. 101 (1996) 191.
[9] R.J. Madix, J. Falconer, A. Suzko, Surf. Sci. 54 (1976) 6.
[10] M. Bowker, Y. Li, Catal. Lett. 10 (1991) 249.
[11] Y. Li, M. Bowker, J. Catal. 142 (1993) 630.
[12] Y. Li, M. Bowker, Surf. Sci. 285 (1993) 219.
[13] Y. Li, M. Bowker, in: T. Dines, C.H. Rochester, J. Thomson (Eds.), Catalysis and Surface Characterisation, Royal Soc. Chem., Cambridge, 1992, p. 221.
[14] N. Aas, M. Bowker, J. Chem. Soc. Faraday Trans. 89 (1993) 1249.
[15] M. Bowker, R.J. Madix, Appl. Surf. Sci. 8 (1981) 299.
[16] M. Bowker, R.J. Madix, Vacuum 31 (1981) 711.
[17] S. York, S. Haq, K. Kilway, J. Philip, F. Liebsle, Surf. Sci. 522 (2003) 34.
[18] B. Sexton, Chem. Phys. Lett. 65 (1979) 469.
[19] J. Davis, M. Barteau, Surf. Sci. 256 (1991) 50.
[20] S. Bao, G. Liu, D.P. Woodruff, Surf. Sci. 203 (1988) 89.
[21] P. Baumann, H.P. Bonzel, G. Pirug, J. Werner, Chem. Phys. Lett. 260 (1996) 215.
[22] R. Haley, M. Tikhov, R.M. Lambert, Catal. Lett. 76 (2001) 125.
[23] M. Bowker, R.J. Madix, Surf. Sci. 102 (1981) 542.
[24] M. Bowker, E. Rowbotham, F. Leibsle, S. Haq, Surf. Sci. 349 (1996) 97.
[25] N. Aas, Y. Li, M. Bowker, J. Phys.: Condens. Matter 3 (1991) S281.
[26] See, for instance A. Frost, R.G. Pearson, Kinetics and Mechanism, second ed., Wiley Intern., N.Y., 1961, p. 19.
[27] T. Cassidy, M.D. Allen, Y. Li, M. Bowker, Catal. Lett. 21 (1993) 321.
[28] M. Bowker, T. Cassidy, M.D. Allen, Y. Li, Surf. Sci. 307–309 (1994) 143.
[29] J.W. He, P.R. Norton, Surf. Sci. 195 (1988) L199.
[30] M. Milun, P. Oervan, M. Vajic, K. Wandelt, Surf. Sci. 211 (1989) 887.
[31] T. Matsushima, Surf. Sci. 217 (1989) 155.
[32] M. Nishijama, J. Yoshinobu, T. Sekitani, M. Onchi, J. Chem. Phys. 90 (1989) 5114.
[33] P. Hu, L. Morales de la Garza, R. Raval, D.A. King, Surf. Sci. 249 (1991) 1.
[34] J. Goschnick, M. Wolf, M. Grunze, W.N. Unertl, J.H. Block, J. Loboda-Cackovic, Surf. Sci. 178 (1986) 831.
[35] J. Goschnick, M. Grunze, J. Loboda-Cackovic, J.H. Block, Surf. Sci. 189 (1987) 137.
[36] R.D. Ramsier, Q. Gao, H. Neergard-Waltenburg, J.T. Yates Jr., J. Chem. Phys. 100 (1994) 6837.
[37] T. Matsushima, K. Shobatake, Y. Ohno, K. Tabayashi, J. Chem. Phys. 97 (1992) 273.
[38] J. Goschnick, M. Grunze, W. Unertl, J. Block, J. Loboda-Cackovic, Surf. Sci. 178 (1986) 831.
[39] M. Bowker, P.D.A. Pudney, C.J. Barnes, J. Vac. Sci. Technol. A 8 (2) (1990) 816.
[40] D.A. King, M.G. Wells, Surf. Sci. 29 (1972) 454.
[41] J. McCarty, J. Falconer, R.J. Madix, J. Catal. 30 (1973) 235.
[42] J. Falconer, R.J. Madix, Surf. Sci. 46 (1974) 473.
[43] R. Sharpe, M. Bowker, J. Phys.: Condens. Matter 7 (1995) 6379.
[44] P.A. Redhead, Vacuum 12 (1962) 203.
[45] M. Bowker, Appl. Catal. 160 (1997) 89.
[46] F. Leibsle, S. Haq, B. Frederick, M. Bowker, N.V. Richardson, Surf. Sci. 343 (1995) L1175.
[47] R.A. Bennett, S. Poulston, I. Jones, M. Bowker, Surf. Sci. 401 (1998) 72.
[48] J.-W. He, U. Memmert, K. Griffiths, P.R. Norton, J. Chem. Phys. 90 (1989) 5082.
[49] H. Tanaka, J. Yoshinobu, M. Kawai, Surf. Sci. 327 (1995) L505.